EFFECTS OF PHASE TRANSFORMATIONS ON LASER FORMING OF Ti-6Al-4V ALLOY

Yajun Fan[1], Zhishang Yang[2], Peng Cheng[1], Keith Egland[2], Y. Lawrence Yao[1]
[1]Department of Mechanical Engineering
Columbia University, New York, NY 10027
[2]Technical Center, Caterpillar, Inc, Peoria, IL, 61552

KEYWORDS

Ti-6Al-4V Alloy, Laser Forming, Flow Behavior

ABSTRACT

In laser forming, phase transformations in the heated affected zone (HAZ) take place under steep thermal cycles, and have a significant effect on the flow behavior of Ti-6Al-4V alloy and the laser forming process. In the present work, the α → β transformation during heating is modeled based on the Johnson-Mehl-Avrami (JMA) theory, and the decomposition of β phase, producing martensite α' or lamellae α dependent on cooling rate, is also numerically investigated. The volume fractions of phases are obtained. Consequently, the flow stress of Ti-6Al-4V alloy is calculated by the rule of mixtures based on the phase ratio and the flow stress of each single phase, which is also a function of temperature, strain and strain rate. According to the obtained flow stress data, the laser forming process of Ti-6Al-4V alloy is modeled by finite element method (FEM), and the deformation is predicted. A series of carefully controlled experiments are also conducted to validate the theoretically predicted results.

INTRODUCTION

In the past decades, considerable research has been carried out on the computer modeling of laser forming, however, the application of numerical modeling is limited by lack of precise data of the temperature and strain rate dependent flow stresses of materials. In general, the flow stress data were generally obtained directly from experiments or the constitutive equation based on limited experimental data. The experiment is cumbersome and time consuming, and flow stress data must be obtained under steady temperatures, that is, the experimentally obtained flow stress data are valid only under phase equilibria, and are not accurate under transient phase transformations like in laser forming. With very fast heating and cooling, laser forming is significantly different from other hot working processes, in which steep temperature gradients and thermal cycles lead to severe microstructural changes in heat affected zone (HAZ) within very short time. A methodology (Fan et al., 2004) has been introduced to model flow behavior under transient phase transformations in laser forming, in which flow the contribution of each phase to flow stresses was calculated by the mixture rule based on its volume fraction, and the temperature, strain and strain rate dependent flow stress data of every single phase can be obtained from experiments. The results show that the method predicts flow behavior of low carbon steel under transient phase transformations very well. However, the prerequisite to apply the methodology is that the kinetic details about the microstructural evolution are well known. With recent developments in computer simulation of phase transformations based on the fundamental kinetic and thermodynamic theories, it is possible to introduce those techniques to describe the particular laser forming process.

In this work we seek to quantitatively understand the kinetics of phase transformation during laser forming of Ti-6Al-4V alloy and their influence on flow behavior and deformation. In particular, the α → β phase transformation during rapid heating, the decomposition of the β phase during rapid cooling. During rapid heating, the kinetics of α → β phase transformation have been extensively investigated by other researchers, and the process can be modeled by the modified Johnson-Mehl-Avrami (JMA) equation for non-isothermal process. The decomposition of the β phase during cooling is much more complicated, and the product is martensitic α' or different morphology secondary α phase depending on cooling rates. Ahmed and Rack (1998) investigated the phase transformations during cooling in Ti-6Al-4V alloy, and concluded that the martensitic transformation takes place as cooling rate above 410 K/s. Slower cooling rates lead to diffusion controlled nucleation and growth process of secondary lamellae α into the β grains. The diffusion controlled β → α phase transformation during cooling is also able to be modeled by JMA equation (Malinov et al., 2001).

The objective of this work is therefore to investigate the phase transformations during laser forming of Ti-6Al-4V alloy and their effects on the alloy flow behavior and forming process, and present a thermal-mechanical-microstructure model for the complex laser forming process with rapid heating and cooling. To validate the theoretically predicted results, a series of carefully controlled experiments are also conducted, and the experimental and numerical results are in close agreement.

MATERIALS AND EXPERIMENTAL PROCESUDRES

Materials

Ti-6Al-4V alloy is an (α + β) two-phase alloy with around 6 wt% aluminum stabilizing the α phase and about 4 wt% vanadium stabilizing the β phase. At room temperature, the microstructure at equilibrium consists mainly of primary α phase (hcp) with some retained β phase (bcc).

A commercial grade Ti-6Al-4V alloy is used in the present work and its chemical composition is shown in Table. 1. The β transus temperature for this material is about 1273 K. As received plate of 0.8 mm thickness in the mill annealed condition were used for testing. It consisted of equiaxed alpha with some amount of intergranular β. The initial volume fraction of β phase was measured by X-ray diffraction (XRD).

TABLE 1 CHEMICAL COMPOSITION OF Ti-6Al-4V ALLOY IN WEIGHT PERCENT.

Al	V	Fe	C	N	O	Ti
6.24	3.98	0.40	0.01	0.05	0.20	Bal.

Experiment

First of all, the starting microstructure of the Ti-6Al-4V alloy used in the present study was tested by XRD. The specimens for XRD, approximately 5 × 5 mm^2, were ground and polished on the surface to be examined.

Ti-6Al-4V alloy plates of 80×80×0.8mm^3 (shown in FIG.1) were then laser scanned straight along the center line (X direction) under different conditions: 1000W & 60mm/s and 500W & 30mm/s, maintaining spot size 6 mm diameter. To enhance laser absorption by the plates, a graphite coating was applied to the surface exposed to the laser. The laser system used was a PRC 1.5 kW CO_2 laser with TEM_{00} mode.

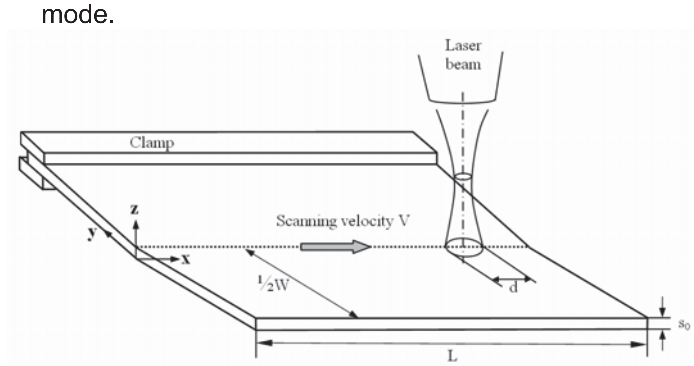

FIGURE 1 SCHEMATIC OF STRAIGHT-LINE LASER BENDING OF Ti-6Al-4V SHEET

After scanning, the bending angles of the formed plates were measured by a coordinate-measuring machine (CMM). The plates were cross-sectioned perpendicular to the scanning path, polished and etched. The changes of macro and micro structures in the HAZ were observed under scanning electron microscopy (SEM).

MATHEMATICAL MODELING

Phase Transformations

During heating, the phase transformation α → β takes place when temperature is increased up to the starting point of the transformation, and then the β phase grows at the expense of the α phase, eventually reaching 100% β phase at the β transus temperature, approximate 1273 K. The α → β transformation in Ti-6Al-4V alloy involves the nucleation of the β phase from the α matrix and the growth of the β phase by diffusion. Therefore, the JMA equation is applicable to describe the α → β transformation in Ti-6Al-4V alloy. This equation is expressed as (Malinov et al., 2001):

$$\frac{f_\alpha(t)}{f_\alpha^{max}} = (1-\exp[-\{k\sum_{i=1}\Delta t_i\}^n])f_\alpha^{ini} \quad (1)$$

where $f_\alpha(t)$ is the amount of α phase after a time t, f_α^{ini} is the initial volume fraction of the α phase of the as received alloy which is measured by XRD, f_α^{max} is the maximum volume fraction of the α phase at the corresponding temperature of the transformation, k is the reaction rate constant and n the Avrami index.

During cooling, the product of the β phase decomposition could be secondary α or martensitic α' depending on cooling rates. The critical cooling rate is around 410 K/s. When cooling rate is less than the critical cooling rate, the transformation is a diffusion controlled nucleation and growth process of secondary lamellae α, and it is also valid to model the transformation by JMA theory. When cooling rate is higher than the critical cooling rate, the β phase will transformed to martensitic α'. For the diffusionless transformations, the amount of martensite $f_{\alpha'}$ is calculated by an empirical formula (Trivedi, 1970):

$$f_{\alpha'} = f_\beta^{'}(1-\chi\exp\{-(M_S - T)\}) \quad (2)$$

where M_S is the martensitic transformation starting temperature, χ is material constant. It has been shown that around 10% β phase retained independent on cooling rate as β phase was cooled to room temperature (Malinov et al., 2001). Therefore, the value of χ is made to be 0.003.

The values of the reaction rate constant k and the Avrami index n during heating and cooling largely depend on the temperature and the mechanism of the transformation, and are not readily available. Malinov et al. (2001) investigated the α ↔ β transformation kinetics of Ti-6Al-4V alloy and gave the values of k and n under different transformation mechanisms at different temperatures, and their result was applied in the present work.

Flow Stress

During laser forming, phase transformations take place in the HAZ and each present phase also undergoes work hardening and softening of dynamic recovery and recrystallization. Therefore, the strategy to model flow behavior is to calculate the flow stress of each single phase, which is also a function of temperature, strain and strain rate, and then sum up the contribution of each phase by the rule of mixtures (Fan et al., 2004):

$$\sigma_{total} = \sum_{j=1}^{N} f_j \sigma_j \quad (3)$$

where σ_{total} is the total flow stress, and f_j and σ_j are the volume fraction and the flow stress of the j^{th} phase of the material, respectively. The information of phase ratio came from the modeling of phase transformation during heating and cooling, and the constitutive relations for the individual α and β phases can be fitted using a variety of flow stress measurement. The constitutive relation for the single α phase of Ti-6Al-4V alloy with equiaxed microstructures could be expressed by the following Eq. 1(Semiatin et al., 2002):

$$\sigma_\alpha^{4.6} = K_\alpha \exp(\frac{273000}{RT}) \times \dot{\varepsilon} \quad (4)$$

where R, T and $\dot{\varepsilon}$ are the gas constant, temperature and strain rate, respectively. The strength coefficient K_α represents the effect of the alloying elements, and the value is about 0.086 for the alloy in the present study. Similarly, the constitutive relation of the single beta phase was expressed as (Semiatin et al., 2002):

$$\sigma_\beta^{4.2} = K_\beta \exp(\frac{160000}{RT}) \times \dot{\varepsilon} \quad (5)$$

in which the strength coefficient K_β = 6.3. The equation (4) and (5) was obtained from the data fitting using a variety of flow-stress measurements within the temperature range around from 1000 K to 1300 K, and flow stress almost remains constant when temperature is above 1300 K. For Ti-6Al-4V alloy, most of deformation takes place as the temperature is above 1000 K with very rapid heating and cooling during laser forming. Therefore, it is assumed that the Equations (4) and (5) are valid for the whole temperature range in the present study.

Thermal-Microstructural-Mechanical Modeling

The heating and deformation during laser forming are both symmetrical about the laser scanning path; therefore only half of the plate (80×40×0.8 mm^3) is modeled in the current research. The temperature field and thermal cycle are calculated from the 3-D thermal FEM modeling, and then the calculated temperature is input into the phase transformation model to get the volume fraction of each phase at a given time step. Because the phase transformation model and grain evolution model require very fine grids to ensure enough accuracy, all phase transformation and grain evolution simulations are only carried out on a cross section perpendicular to the scanning path of the plate. This is reasonable considering that all points along the scanning direction undergo similar thermal cycles and deformations. The flow stresses are calculated based on the phase volume fractions from phase transformation modeling. Finally, the temperature field and flow stresses are input into the mechanical model to calculate the thermal strain and predict the deformation. A commercial code, ABAQUS, was used to model the decoupled thermal and mechanical process. In mechanical analysis, C3D20 element was applied, and the phase transformation and flow stress were calculated in the subroutine UHARD.

Two cases were run in the current research: P = 1000 W & V = 60 mm/s, and P = 500 W & V = 30 mm/s, where P represents power and V is scanning velocity. In both cases, the laser beam spot size is 6 mm in diameter.

RESULTS AND DISCUSSIONS

Initial Phase Ratio

The initial phase ratio of the α and β phases was measured by XRD. In the obtained XRD pattern, the diffraction lines α (101) and β (110) were chosen to make quantitative analysis using direct comparison method. According to the direct comparison method, we can obtain the following relationship:

$$\frac{I_\beta}{I_\alpha} = \frac{Af_\beta}{f_\alpha} = \frac{A(1-f_\alpha)}{f_\alpha} \qquad (6)$$

where f_α is the initial volume fraction of the α phase, f_β is the initial volume fraction of the β phase, I_α and I_β are the measured integrated intensities corresponding to the α (101) and β (110) peaks, respectively. The constant A was calculated to be about 1.67, therefore, the parameters f_α and f_β are calculated to be 0.75 and 0.25, respectively.

Macro- and Micro- structures from Experiments

FIG. 2 shows the SEM images of part of the laser formed cross section perpendicular to the scanning path. A distinctly darkened region is observed. The darkened sub-region is the heat affected zone (HAZ), where phase transformation took place but no melting was involved. The size of HAZ is measured to compare with the numerical results.

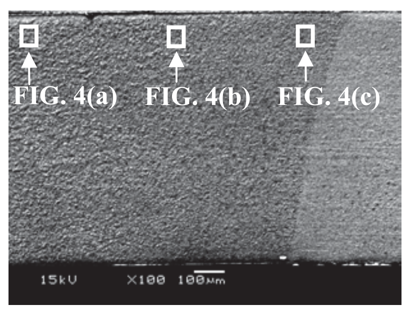

FIGURE 2 SEM IMAGINE OF THE CROSS SECTION PERPENDICULAR TO THE SCANNING PATH. The HAZ AND HAZ BOUNDARY WERE OBSERVED: POWER=1000W, AND SCANNING VELOCITY = 60 mm/s.

FIG. 3 shows the microstructures at three different locations on the top surface in the HAZ under the conditions of 1000W & 60mm/s. In FIG. 3 (a), martensite α’ is observed in the centre of the HAZ close to the scanning line. The α’ phase is composed of long orthogonally oriented martensitic plate having an acicular morphology, and a substructure containing predominately dislocations and stacking faults with a few platelets containing twins. Clearly, α’ is the dominant phase at the centre of the HAZ, where the material experienced a very high cooling rate. FIG. 3 (b) shows that the main phase in the middle of the HAZ is the secondary Widmanstatten α, and this α morphology has a blocky appearance with a heavily dislocated internal substructure. A small amount of primary α is also observed from the SEM image. This primary α phase is the remained in transitional region after the α→ β transformation during heating. In the area close to the boundary of HAZ, the amount of the remained primary α increases and the block of the secondary α is smaller, which can be seen from FIG. 3 (c). The case of 500W & 30 mm/s shows an identical phase distribution within the HAZ.

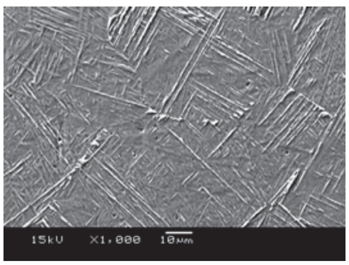

(a)

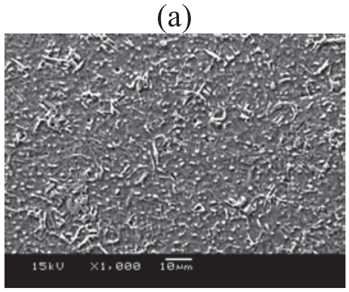

(b)

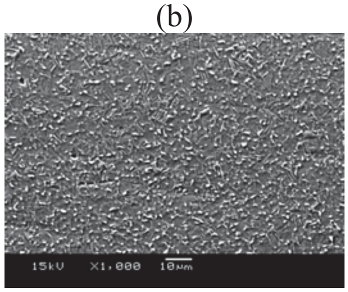

(c)

FIGURE 3 MICROSTRUCTURES AT DIFFERENT LOCATIONS IN THE HAZ ALONG Y DIRECTION AFTER LASER SCANNING, 100 W AND 60 mm/s: (a) CLOSE TO THE SCANNING PATH (HEAT SOURCE); (b) FAR FROM THE SCANNING PATH, AND (c) FURTHER FROM THE SCANNING PATH, AND CLOSE TO THE HAZ BOUNDARY.

Based on the experimental observation, the HAZ experienced significant phase transformations during the laser forming, as a result, the martensite α’ was substantially formed due to high cooling rate in the center of the HAZ, and in the area further from the scanning line, the blocky secondary α was produced under a lower cooling rate. Some retained primary α was also found in the area close to the HAZ boundary. A small amount of retained β should also be produced in the HAZ, but it is generally in the form of thin film between martensite α’ or secondary α plates, and can not be observed from the SEM imagines.

Modeling of Phase Transformations

The calculated thermal cycles at different locations on the top surface of the scanned plate, obtained from FEM thermal model, are shown in FIG. 4. The figure shows that the heating rate and the cooling rate were very large, and the magnitude of heating rate was up to 4×10^4 K/s.

The phase transformation during heating is relatively simple because no melting is involved and only the α → β transformation is considered. The process was predicted by the JMA equation. When the heating process has just finished and the cooling process is about to start, which is assumed to be when the peak temperature was reached, the calculated volume fractions of primary α and β are taken as the initial conditions for phase transformation during cooling.

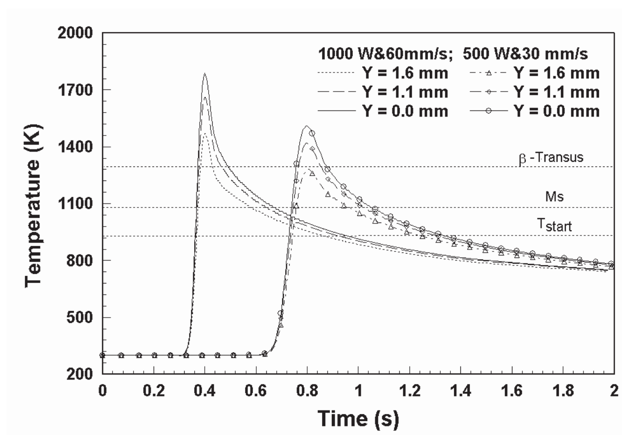

FIGHRE 4 THE CALCULATED THERMAL CYCLES AT DIFFERENT LOCATIONS ALONG Y DIRECTION ON THE TOP OF THE HAZ AS X=20mm, FROM FEM THERMAL MODELING OF LASER FORMING OF Ti-6Al-4V ALLOY

Upon heating, The temperature where the dissolution of the primary α and the formation of the β phase start to take place was assume to be T_{start} for this Ti-6Al-4V alloy, therefore, Between the temperature T_{start} and the β transus temperature, primary α and transformed β coexisted and formed a transitional region. 100% β phase was obtained when temperature was above the β transus line (shown in FIG. 4). The values of T_{start} and the β transus are dependent on chemical composition of alloy and superheating, which causes the temperatures shift toward up. The value of T_{start} is around 913±30 K and the β transus is about 1243±50 K. In this model, the values of T_{start} and the β transus were given 940 and 1273, respectively. In reality, T_{start} and the β transus are different during heating and cooling due to superheating and undercooling, however, in phase transformation model T_{start} and the β transus were fixed during both heating and cooling. The effect of superheating and undercooling can be considered from the difference of the values of n and k between during heating and cooling. The calculated β phase distributions at the end of the heating process (the points on the scanning line reached its peak temperature) for both cases are shown in FIG. 5. The contours in FIG. 5 show that the HAZ region in the case of 1000W & 60mm/s is larger than that in the case of 500W & 30mm/s because a less energy loss. The comparison between the experimentally obtained and the calculated HAZ size is also given in Table 2. The comparison shows that the numerical result is in good agreement with the experimentally obtained HAZ size.

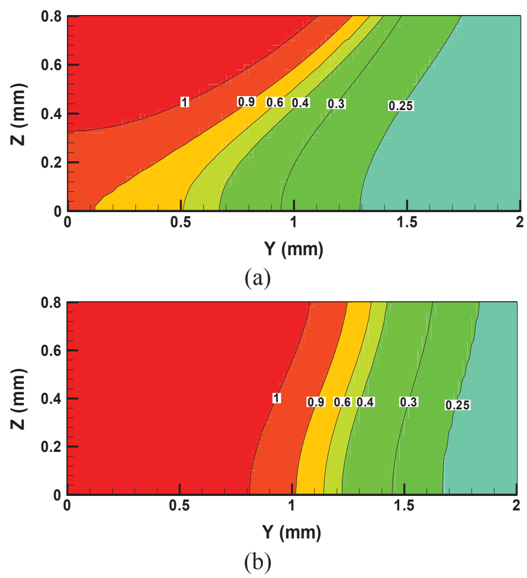

FIGURE 5 THE DISTRIBUTION OF VOLUME FRACTION OF β PHAES AT THE END OF HEATING IN THE CROSS SECTION AREA PERPENDICULAR TO SCANNING PATH, ONLY HALF OF THE AREA WAS MODELED DUE TO SYMMETRY ABOUT Y: (a) P=500W, V=30mm/s; AND (b) P=1000W, V=60mm/s.

TABLE 2 COMPARISON OF HAZ SIZE BETWEEN EXPERIMENTAL AND NUMERICAL RESULTS

	HAZ top half-width (mm)		HAZ bottom half-width (mm)	
	Exp.	Num.	Exp.	Num.
500 W & 60 mm/s	1.73 ± 0.05	1.76	1.32 ± 0.03	1.29
1000 W & 60 mm/s	1.83 ± 0.02	1.80	1.64 ± 0.02	1.67

To quantitatively predict the decomposition of the β phase in the HAZ during cooling, the cooling rates were first calculated from the 3D FEM thermal modeling, and then judged whether the diffusion controlled β → α transformation or the martensitic transformation would take place, and determined equation (2) or (3) was used. The calculated phase distributions after laser forming in the conditions of 1000W & 60mm/s are given in FIG.6. From FIG.6 (a), the primary α in the transitional region was retained during the cooling process, and no changes happened to the volume fraction of primary α after heating. FIG. 6(b) shows the volume fraction of martensitic α' formed in cooling. In the area close to heat source, the cooling rate is higher, and a substantial amount of martensite was formed. It must be emphasized, however, that for all cooling rates, a small amount of residual β phase remained after cooling. It amount was found to be 9±2 wt pct, and the amount of residual β phase was independent on cooling rate. In the current model, the residual β phase was assumed to be 10 %. So in the area close to heat source, the phases were composite of (90% α'+10% β). Even in the transitional region, some β phase transformed to martensite. The closer to the HAZ boundary, the lower the cooling rates were. When cooling rates were under the critical rate, martensitic transformation stopped, and the diffusion controlled β → α transformation took place. That was why the volume fraction of martensite in the region close to the HAZ boundary was zero. FIG. 6 (c) shows the distribution of secondary α. The secondary α was only the product of the diffusion controlled β → α transformation, which took place under lower cooling rates. FIG 6 (d) shows the distribution of β phase. In the region where martensitic transformation took place, the residual β phase is around 10 %, and then gradually reduced with the β → α transformation, and outside the HAZ, the β phase remained the initial 25% volume fraction. Because the phase transformation mechanism in the region of martensitic transformation is different from the mechanism in the region of the diffusion controlled $\beta \rightarrow \alpha$ transformation, the volume fraction of residual β is discontinuous across the two regions. Similar numerical results are obtained in the case of 500W & 30mm/s, and only the size of phases regions are different.

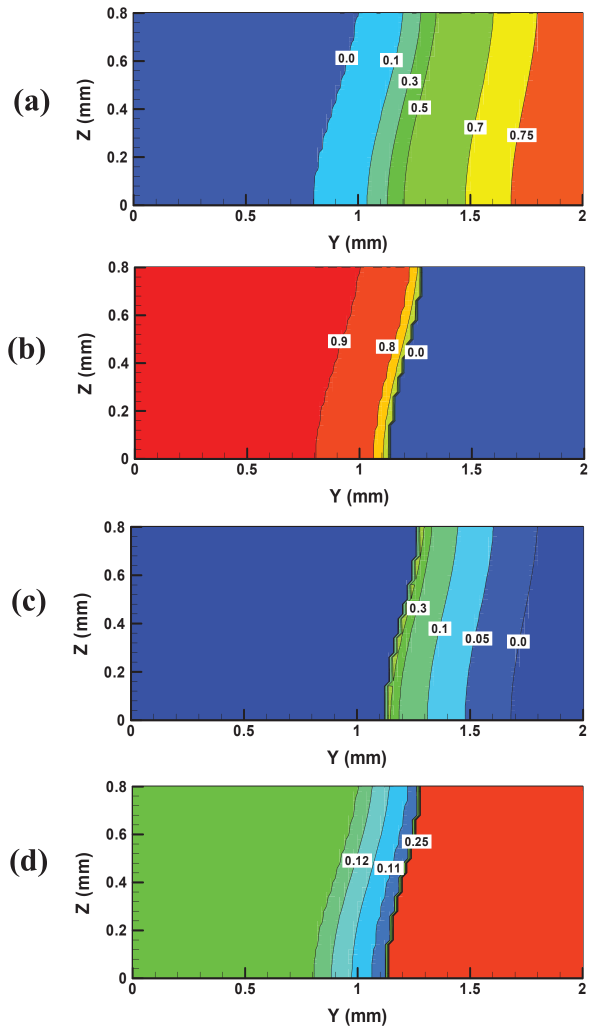

FIGURE 6 THE CALCULATED PHASE DISTRIBUTION AFTER COOLING, ONLY HALF OF THE AREA WAS MODELING DUE TO SYMMETRY ABOUT Y, P= 1000 W AND V = 60 mm/s: (a) PRIMARY α, (b) MARTENSITE α', (c) SECONDARY α, and (d) β

From the modeling, the final phase constitution after very steep thermal cycles during laser forming includes martensite α', remained primary α, secondary α and a small amount of retained β in the HAZ. In fact, the secondary α can be divided into Widmanstatten and basketweave structure based on their morphology. The flow behavior of Ti-6Al-4V alloy are also affected by the morphology and texture, but because the deformation mainly took place when temperature was above 1000 K and only lasted very short time, their effects on the deformation were greatly limited under high temperature. Therefore, the effect of the morphology and texture of the α phase on flow stress were neglected.

Deformations

After the real time phase constitutive information is obtained by the phase transformation modeling, the flow behavior can be calculated by the rule of mixtures (Eq. (3)). Based on the calculated transient flow stress and the FEM mechanical modeling of laser forming, the bending angles of the plates can be predicted. The bending angles were also experimentally obtained. In the experiments of laser forming, it was found that the temperature gradient mechanism was active for both cases despite the large laser beam diameter to sheet thickness ratio. This was attributed to the low thermal conductivity of the titanium alloy. FIG. 7 shows that the experimental and the numerical results of the bending angles along the scanning path agree with each other very well when the effect of transient phase transformations on flow behavior was considered. It can be seen that, from the entering end of the scanning path (X = 0 mm), the bending angle first drops a little and then increases to a greater angle at the exiting end. This phenomenon is called the edge effect and was already investigated in detail in an earlier research (Bao and Yao, 1999). The drop of the bending angle after the laser enters the plate is caused by the stronger surrounding constraint in the middle of the plate. The bending edge curvature is dependent on the bending mechanism, constraint by the surrounding material and preheating. In the case of 1000W & 60 mm/s, the scanning velocity was faster that in the case of 500W & 30 mm/s, and it was expected that the exiting end was preheated to a less extent. For Ti-6Al-4V alloy, however, the faster speed could not cause large difference on heat accumulation at the exiting end due to its very low thermal conductivity. In contrast, the higher input energy in the case of 1000W & 60 mm/s caused easy buildup at the exiting end. Therefore, the increase of the bending angle at the exiting end was larger in the case of 1000W & 60mm/s than that of the 500W & 30mm/s case. Similarly, the bending edge curvature in the case of 1000W & 60mm/s was larger. To show the difference between with and without the consideration of transient phase transformations, numerical modeling was also run by directly input flow stress data, from literature (Seshacharyulu et al., 2000), as a tabular function of the equivalent strain, strain rate and temperature, that is, the modeling did not consider the effect of transient phase transformations on flow stress. The numerical results are also shown in FIG. 7. Obviously, the numerical results with phase transformation consideration match the experimental results better.

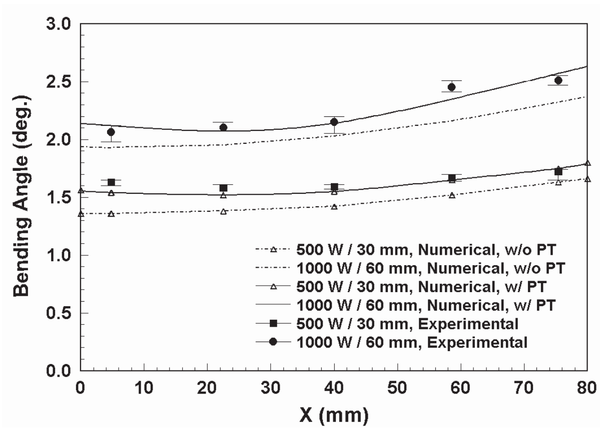

FIGURE 7 THE COMPARISON OF NUMERICALLY PREDICTED BENDING ANGLES W/ AND W/O PHASE TRANSFORMATION CONSIDERATION (PT) WITH EXPERIMENTAL RESULTS AT VARIOUS LOACTIONS ALONG SCANNING PATH (Y=0 mm).

CONCLUSIOINS

A thermal-microstructural-mechanical model has been developed for the laser forming process. The model considers the effect of phase transformations on then flow behavior of Ti-6Al-4V alloy. The phase transformation of Ti-6Al-4V alloy during laser forming was modeled based on the phase transformation kinetics, and the final phases concludes martensite α' and secondary α except the β and remained primary α. A large amount of martensite α' was formed in the area close to scanning path (heat source). According to comparison of the HAZ macrostructure, phase constitution, and bending angle between the experimental and numerical results, the proposed model is able to predict the microstructure evolution and the deformation caused through laser forming well.

ACKNOWLEDGEMENTS

The work is supported by NIST under grant ATP-00005269.Discussion with and some material data provided by Dr. Judson Marte of General Electric Global Research Center are also gratefully acknowledged.

REFERENCES

Fan, Y., Yang, Z., Cheng, P., Egland, K., and Yao, Y. L., (2004), "Numerical and Experimental Investigation of Microstructure Evolution and Mechanical Behavior of Steel in Laser Forming," *ASME J. Manuf. Sci. Eng.*, submitted.

Ahmed, T. and Rack, H. J., (1998), "Phase Transformations during Cooling in α + β Titanium Alloys," *Mat. Sci. & Eng.*, Vol. A243, pp. 206-211.

Malinov, S., Markovsky, P., Sha, W. and Guo, Z., (2001),"Resistivity Study and Computer Modeling of The Isothermal Transformation Kinetics of Ti-6AL-4V and Ti-6Al-2Sn-4Zr-2Mo-0.08Si Alloys," *Journal of Alloys and Compounds*, Vol. 314, pp. 181-192

Trivedi, R., (1970), "Growth of Dendritic Needles from a Supercooled Melt," *Acta Met*, Vol. 18(3), pp. 287-296.

Semiatin, S. L., Montheillet, F., Shen, G. and Jonas, J.J., (2002),"Self-Consistent Modeling of the Flow Behavior of Wrought Alpha/Beta Titanium Alloys under Isothermal and Nonisothermal Hot-working Conditions," Metal*. and Mat. Trans. A*, Vol. 33A, pp.2719-2727.

Bao, J. and Yao, Y. L., (1999), "Study of Edge Effects in Laser Bending," *Proceeding ASME IMECE 1999*, MED-10, pp. 941-948.

Seshacharyulu, T., Medeiros, S. C., Frazier, W. G., and Pradad,. Y. V. R. K., (2000), "Hot Working of Commercial Ti-6Al-4V with an equiaxed α – β Microstructure: materials modeling considerations," *Mat. Sci. and Eng.*, Vol. A284, pp. 184-194.